FRACTAL MODELS ARE INADEQUATE FOR THE KINETICS OF FOUR DIFFERENT ION CHANNELS

O. B. McMANUS,* D. S. WEISS,* C. E. SPIVAK,‡ A. L. BLATZ,§ AND K. L. MAGLEBY*
*Department of Physiology and Biophysics, University of Miami School of Medicine, Miami, Florida 33101; ‡National Institute on Drug Abuse, Addiction Research Center, Baltimore, Maryland 21224; and §Department of Physiology, University of Texas Southwestern Medical Center, Dallas, Texas 75235

ABSTRACT The gating kinetics of single ion channels have been well described by models which assume that channels exist in a number of discrete kinetic states, with the rate constants for transitions among the states remaining constant in time. In contrast to such discrete Markov models, it has recently been considered whether gating might arise from transitions among a continuum of states, with the effective rate constants for leaving the collections of states given by a fractal scaling equation (Liebovitch, L. S., J. Fischbarg, J. P. Koniarek, I. Todorova, and M. Wang. 1987. *Biochim. Biophys. Acta.* 896:173–180; Liebovitch, L. S., and J. M. Sullivan. 1987. *Biophys. J.* 52:979–988). The present study compares discrete Markov with fractal continuum models to determine which best describes the gating kinetics of four different ion channels: GABA-activated Cl channels, ACh-activated end-plate channels, large conductance Ca-activated K (BK) channels, and fast Cl channels. Discrete Markov models always gave excellent descriptions of the distributions of open and shut times for all four channels. Fractal continuum models typically gave very poor descriptions of the shut times for all four channels, and also of the open times from end-plate and BK channels. The descriptions of the open times from GABA-activated and fast Cl channels by the fractal and Markov models were usually not significantly different. If the same model accounts for gating motions in proteins for both the open and shut states, then the Markov model ranked above the fractal model in 35 of 36 data sets of combined open and shut intervals, with the Markov model being tens to thousands of orders of magnitude more probable. We suggest that the examined fractal continuum model is unlikely to serve as a general mechanism for the gating of these four ion channels.

INTRODUCTION

Ion channels are large integral membrane proteins which allow passive flux of ions through cell membranes (Hille, 1984). Currents recorded from ion channels with the patch clamp and bilayer techniques (Hamill et al., 1981; review by Miller, 1983) have shown that ion channels repeatedly open and close, or gate their pores, during normal activity. The gating mechanism is of considerable interest because of the dominant role channels play in the control of membrane potential and other key cellular processes (Hille, 1984). Models for the gating of ion channels have generally assumed that the channels exist in a limited number of discrete open and shut states, with the rate constants for transitions among the various states remaining constant in time (Colquhoun and Hawkes, 1981). Such discrete Markov models account for many of the complex features of single channel kinetics (Magleby and Pallotta, 1983; Moczydlowski and Latorre, 1983; Aldrich et al., 1983; Horn and Vandenberg, 1984; Colquhoun and Sakmann, 1985; Labarca et al., 1985; Blatz and Magleby, 1986*b*; Sine and Steinbach, 1987; Kerry et al., 1988). In marked contrast to Markov models with a limited number of discrete kinetic states, it has recently been considered that the open and shut states may each be represented by a continuum of states, with the effective rate constants for leaving the collection of open and shut states given by a fractal scaling equation (Liebovitch et al., 1987; Liebovitch and Sullivan, 1987).

In a detailed examination of the fractal continuum model, McManus and Magleby (1988) have found that it cannot describe the single channel kinetics of a large conductance Ca-activated K channel (BK channel). The purpose of this present study is to extend the examination of the fractal continuum model to three other types of channels, present additional findings for the BK channel, and summarize the results for all four channels. Sufficient data with high time resolution are obtained so that the predictions of the examined models can be critically assessed. The findings indicate that the examined fractal continuum model is unlikely to serve as a general gating mechanism for the four studied ion channels. A preliminary report of this work has appeared (Magleby et al., 1988).

PREDICTED CHANNEL KINETICS

Discrete Markov Model

Discrete Markov models assume that channel gating is associated with transitions among a limited number of

Present address of Dr. McManus is Merck, Sharp & Dohme Research Laboratories, R80B19, P.O. Box 2000, Rahway, NJ 07065.

open and shut states or conformations, with the rate constants for the transitions remaining constant in time. Such models predict that the distributions of open and shut interval durations will each be described by the sums of exponentials, with one exponential component for each state, although all components may not be detected experimentally (Colquhoun and Hawkes, 1981). Thus, distributions generated by discrete Markov models should be described by

$$f(t) = \sum_{j=1}^{k} a_j \tau_j^{-1} e^{-t/\tau_j}, \quad (1)$$

where $f(t)$ is the probability density function (PDF), k is the number of exponential components, and τ_j and a_j are the time constant and area, respectively, of each component j.

The number of free parameters for the Markov model is given by

$$FP_M = 2k - 1, \quad (2)$$

where k is the number of exponential components. Since the areas of the exponential components must sum to 1.0 for a PDF, one of the areas is not a free parameter. Consequently, for a single exponential component there is only one free parameter (the time constant), and for each additional exponential component after the first there are two additional free parameters (an area and time constant).

Fig. 1 *A*, which plots on log-log coordinates the number of intervals versus their duration, presents some examples of the types of distributions expected for discrete Markov gating kinetics. If there is a single shut (or open) state, then the distribution of intervals would be described by a single exponential (*continuous line*). If there are multiple states, then the observed distributions would depend on the magnitudes and time constants of the exponential components generated by the states. For some sets of rate constants, each state will lead to a discrete bump in the distribution, as shown by the dotted line generated by a model with three shut states. For other sets of rate constants, the distribution could appear as a straight line, or power type relationship, as shown by the dashed line generated by a model with seven shut states. The shapes of distributions which can be generated by discrete Markov models, including combinations of smooth lines for some parts of the distribution and bumps and inflections in other parts, is endless, depending only on the underlying rate constants for the transitions between the various states.

Fractal Continuum Model

The fractal continuum model assumes that the distributions of open and shut intervals are described by the empirical equation

$$f(t) = At^{1-D} \exp\{-[A/(2-D)]t^{2-D}\}, \quad (3)$$

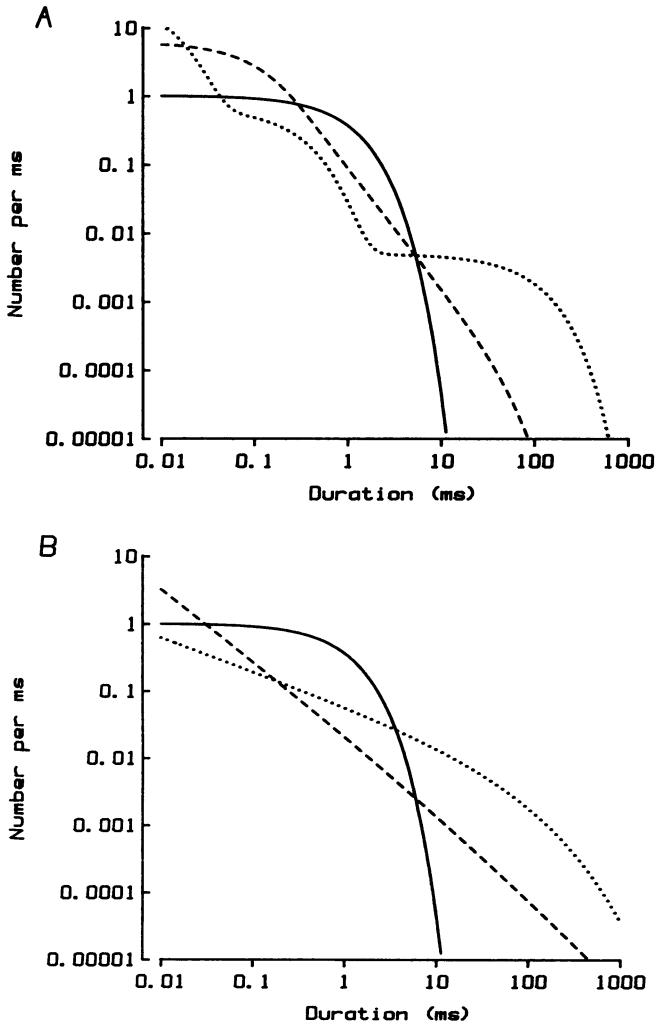

FIGURE 1 Predicted distributions of interval durations for discrete Markov models and the fractal continuum model. Numbers of intervals are plotted against interval duration of log-log coordinates, in the form of probability density functions. (*A*) Markov model with: *continuous line*, single exponential with time constant of 1 ms and area of 1; *dotted line*, sum of three exponentials with time constants (and areas) of: 0.01 ms (0.3), 0.3 ms (0.2), and 100 ms (0.5); *dashed line*, sum of seven exponentials with time constants (and areas) of: 0.1 ms (0.504), 0.25 ms (0.252), 0.625 ms (0.126), 1.56 ms (0.063), 3.91 ms (0.0315), 9.76 ms (0.0157), and 24.4 ms (0.00787). (*B*) Fractal model with: *continuous line*, $A = 1$ Hz and $D = 1$; *dotted line*, $A = 2\ \text{Hz}^{0.5}$, $D = 1.5$; *dashed line*, $A = 0.5\ \text{Hz}^{0.1}$, $D = 1.9$.

where A is the kinetic setpoint, and D is the fractal dimension, such that $1 \leq D < 2$ (Liebovitch et al., 1987; Liebovitch and Sullivan, 1987). The fractal continuum model has only two free parameters for each distribution, A and D.

One proposed interpretation of Eq. 3 is that channel gating is associated with transitions among a continuum of open and shut conformational states, with the effective rate constants for leaving the open or shut states being a mixture of the rate constants for leaving the collection of states (Liebovitch and Sullivan, 1987). Although Liebo-

vitch and Sullivan (1987) do not derive how such a physical model could lead to the empirical Eq. 3, Millhauser et al. (1988) and Laüger (1988) have presented models with a large number of states with similar rate constants for the transitions among the states, which could provide a physical basis for apparent fractal scaling as D approaches two.

Fig. 1 *B* presents some examples of the types of distributions expected for the fractal continuum model described by Eq. 3. If the fractal dimension D equals one, then the distribution of intervals would be described by a single exponential (*continuous line*). When D approaches two, a power type distribution is generated (*dashed line*). Intermediate values of D give intermediate distributions (*dotted line*, $D = 1.5$). In no case does the fractal continuum model predict discrete bumps or inflections in the distribution. Thus, whereas both discrete Markov models and the fractal continuum model can generate smooth distributions which can range from a single exponential to a power type function, only discrete Markov models can generate discrete bumps and inflections in the distributions.

METHODS

The patch clamp recording technique (Hamill et al., 1981) was used to record single channel currents from four different ion channels.

GABA-activated Channel

Currents were recorded from GABA-activated channels in excised inside-out membrane patches from 5–10-d-old cultures of chick cerebral neurons. Briefly stated, cerebral hemispheres were removed from stage 34 white Leghorn chicks and dissociated by extrusion through a 44-μm pore nylon mesh. The cells (predominately neurons) were then plated and cultured. Further details are in Weiss et al. (1988). The solution in the patch pipette contained (mM): choline chloride, 130; $CaCl_2$, 2; $MgCl_2$, 1; Hepes-TEAOH, 10; GABA, 1 μM; pH 7.4. The solution at the intracellular membrane surface contained (millimolar); choline chloride, 130; EGTA, 1; $MgCl_2$, 1; Hepes-TEAOH, 10; pH 7.4.

Fast Cl Channel

Currents were recorded from Cl channels with fast kinetics in excised, inside out membrane patches from primary cultures of rat skeletal muscle (myotubes). Complete details are in Blatz and Magleby (1986*b*). The solution bathing the outer membrane surface (the solution in the patch pipette) contained (mM): KCl, 140; TES buffer, 5; EGTA, 0.5; and sufficient added Ca^{2+}, for a free Ca^{2+} of 10^{-8}–10^{-9} M. The solution bathing the inner membrane surface contained (mM): KCl, 1,000; TES buffer, 2–5; and no added Ca^{2+}; pH 7.2; temperature was either 7.6 or 20°–22°C. The high concentration of Cl^- was used to increase the amplitudes of the single-channel currents, increasing the signal-to-noise ratio.

End-Plate Channel

Currents were recorded from end-plate activated channels in cell attached patches from end-plate regions of interosseal muscles dissected from the toes of the frog *Rana pipiens*. The muscles, in a 10-ml beaker, were treated with 5 mg/ml (1–2 ml) of collagenase (Type I; Sigma Chemical Co., St. Louis, MO) plus tetrodotoxin (1 μM) for 30 min. Then protease (Type VII, 0.5 mg/ml; Sigma Chemical Co.) was added (total volume ~ 5–6 ml), and the incubation continued for another 30–75 min. The muscles were shaken during the above procedures on an orbital shaker with just enough force to keep the muscles suspended and in gentle motion. To end the dissociation, the fibers were washed three times with Ringer's solution and then stored in Hepes-buffered Ringers's solution at 5°C. The fibers were used within 2 d. The solution used to bath the muscles contained (mM): NaCl, 116; KCl, 2; Na_2PO_4, 1.3; NaH_2PO_4, 0.7; pH 7.0. The solution in the patch clamp recording pipette contained (mM): NaCl, 116; KCl, 2; Hepes, 2; 0.3 μM tetrodotoxin; and 0.1 μM of either of the agonists isoarecolone methiodide or dihydroisoarecolone methiodide (Waters et al., 1988). The potential in the pipette was adjusted until the single channel current amplitude fell between 4.0 and 4.2 pA. Experiments were performed at 10°–11°C.

Large Conductance Ca-Activated K Channel

Currents were recorded from large conductance Ca-activated K channels (BK channels) in excised inside out membrane patches from primary cultures of rat skeletal muscle (myotubes). Complete details are in McManus and Magleby (1988). The solutions bathing both sides of the membrane contained (millimolar): KCl, 144; TES buffer, 2; and EGTA 1; pH 7.0 or 7.2, temperature, 22°–24°C. Sufficient Ca^{2+} was added to the solution bathing the intracellular membrane surface to bring the free Ca to 0.1–20 μM, depending on the experiment.

Recording and Measuring Intervals

Single-channel currents were stored on FM tape during the experiments. The data on the tape were then actively low pass filtered and analyzed by computer to determine the durations of open and shut intervals. 50% threshold detection was used for the fast Cl, end-plate, and BK channels, as described previously (Blatz and Magleby, 1986*b*; McManua and Magleby, 1988). In this analysis, the data were played into the computer at 1/4 to 1/16 of the normal tape speed. The data were always examined on an oscilloscope as it was played into the computer to look for possible baseline drift and noise artifacts. The baseline was adjusted if necessary and any noise artifacts were noted for later exclusion. Each interval for the GABA-activated and end-plate channels were visually approved and then measured by computer using a 50% threshold for detection (details for GABA-activated channels in Weiss, 1988).

The filtering during analysis was always sufficient to reduce noise peaks in the absence of channel activity to less than the 50% detection level. Such filtering prevents the noise peaks from generating artificial fast components.

Stability plots of mean open and shut durations were used to detect and exclude modes other than normal (Blatz and Magleby, 1986*b*; McManus and Magleby, 1988) and to exclude data with drifting means.

Binning and Plotting Interval Durations

Open and shut intervals were binned according to the logarithms of their durations and plotted on log-log coordinates as frequency histograms, which plot the number of observed intervals versus interval duration (details in McManus et al., 1987). Such plots provide a convenient method to display data that span many orders of magnitude in interval durations and frequency of occurrence. In making the plots, additional bins were sometimes combined further after the log binning to reduce variation in successive plotted points. The numbers of events in each bin were divided by bin width, in order to account for increasing bin width (McManus et al., 1987). The resulting plot is essentially a scaled probability density function, with an area equal to the total number of events that would be contained within the distribution.

Fitting Distributions of Interval Durations with Sums of Exponentials or the Fractal Continuum Model

To assess the ability of discrete Markov models to describe the data, histograms of open and shut interval durations were fit with Eq. 1 using

the method of maximum likelihood (Colquhoun and Sigworth, 1983; with details for fitting log-binned data in McManus et al., 1987). The number of significant exponential components was determined with the likelihood ratio test (Rao, 1973; Horn and Lange, 1983).

To assess the ability of the fractal continuum model to describe the data, the distributions of open and shut intervals were fit with Eq. 3 using the method of maximum likelihood. For fitting with either model, the durations of all intervals less than two times the dead time were excluded from the fitting process, as the durations of these intervals are underestimated (Colquhoun and Sigworth, 1983), and including such intervals can lead to "phantom" exponential components (Roux and Sauvé, 1985; Blatz and Magleby, 1986*a*).

Ranking the Discrete Markov and Fractal Continuum Models

The discrete Markov and fractal continuum models are not nested, that is, one is not a subset of the other. Such non-nested models may be ranked with the prediction error approach (Akaike, 1974; Horn, 1987), which has the limitation that the significance level is not known. To apply this approach, an Akaike predictor value, $P_{M/F}$, was first determined from

$$P_{M/F} = \log_e (L_M/L_F) - (n_M - n_F), \quad (4)$$

where L_M and L_F are the maximum likelihoods that the observed experimental data were drawn from the distributions predicted by the discrete Markov (M) and fractal continuum (F) models, respectively, and n_M and n_F are the number of free parameters for models M and F. If $P_{M/F} > 0$, then model M was ranked above model F, and if $P_{M/F} < 0$, then model F was ranked above model M. If $P_{M/F} = 0$, then the two models are of equal ranking. This ranking procedure places a heavy penalty on free parameters. Starting with equally likely models with equal numbers of free parameters, if each additional free parameter increases the probability less then *e*-fold, then the additional free parameters will lead to a lower ranking.

Determining the Significance of the Akaike Predictor Ranking

The methods detailed in Horn (1987) have been used to determine a level of significance for the ranking provided by the Akaike predictor value. Briefly stated, the data were resampled with the bootstrap method in order to estimate the variability in estimates of the predictor value. Typically, 50 or more artificial data sets were generated from the original data set by resampling with replacement (Efron, 1982) and then fit to determine $P_{M/F}$ for each data set. Each resampled data set was made by drawing at random from the original data set a number of samples equal to the number contained in the original data set. In such a drawing with replacement, some data points are used more than once and some are not selected. Each resampled data set was different because the random numbers used for the drawings were different. The values of $P_{M/F}$ determined from the resampled data sets were then fit with a Gaussian distribution to determine if the resampled data were significantly different from zero ($P < 0.05$).

RESULTS

GABA-Activated Channel

Fig. 2 presents log-log plots of the distributions of open (A) and shut (B) interval durations for data recorded from GABA-activated channels in a single excised membrane patch from cultured chick cerebral neurons. To determine whether these data were more consistent with a discrete Markov model or fractal continuum model for channel

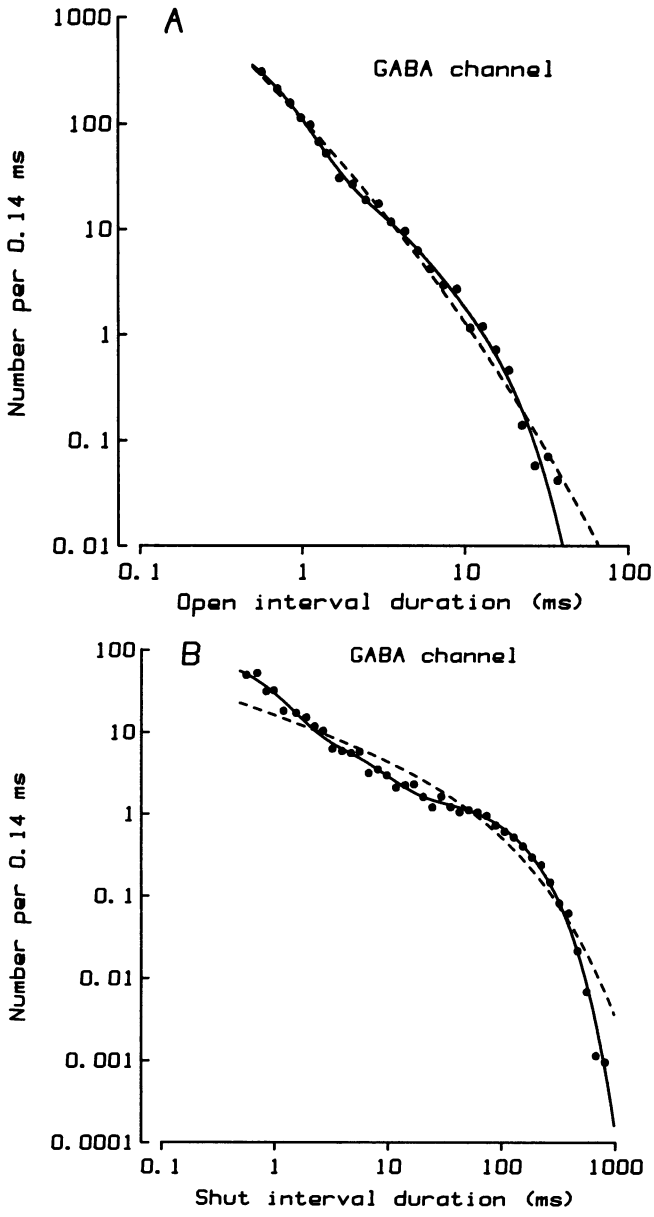

FIGURE 2 Distributions of durations of open and shut intervals recorded from GABA-activated channels fit by Markov and fractal models. The numbers of intervals are plotted against their durations on log-log coordinates. (*A*) Open times. The continuous line plots the maximum likelihood fit to the open interval distribution with the sum of three exponentials, with time constants (and areas in parentheses) of: 0.361 ms (0.771), 1.83 ms (0.140), and 5.87 ms (0.089). The dashed line plots the maximum likelihood fit to the open distribution with the fractal continuum model, with $A = 3.86$ Hz$^{0.21}$ and $D = 1.79$. The exponent on Hz is given by $2 - D$. (*B*) Shut times. The continuous line plots the fit to the shut durations with the sum of three exponentials, with time constants (and areas) of: 0.615 ms (0.209), 4.82 ms (0.159), and 105 ms (0.632). The dashed line plots the fit to the shut durations by the fractal continuum model with $A = 3.10$ Hz$^{0.56}$ and $D = 1.44$. The likelihood ratio for the Markov to the fractal model was e^{25} for the open distribution and e^{139} for the shut. 1,593 open and 1,819 shut intervals were fitted and plotted. The difference between the numbers of open and shut intervals arises because the fractions of intervals less than two dead times in duration, and hence excluded from the fits, are different for the open and shut distributions. Membrane potential = −50 mV; 1.0 μM GABA; dead time = 0.18 ms.

kinetics, the most likely fits to the data with each model were calculated and compared.

The continuous lines in Fig. 2, plot the best description of the data with a discrete Markov model (Eq. 1, sums of exponentials). The discrete Markov model gave an excellent description of the observed interval durations, including the inflections in the histograms. The dashed lines in Fig. 2 plot the best description of the plotted data with the fractal continuum model (Eq. 3). The fractal model only approximated the data, as it could not describe the inflections. Since inflections are never predicted by the fractal model (Fig. 1 and Liebovitch et al., 1987), the fractal model appears inconsistent with the data.

The Likelihood Ratio Indicates That the Discrete Markov Model Is More Probable. A quantitative measure of the difference in ability of the discrete Markov and fractal continuum models to describe the data was obtained from the likelihood ratio, L_M/L_F, which is the likelihood that the observed data were drawn from the distributions described by the discrete Markov model, divided by the likelihood that the observed data were drawn from distributions described by the fractal continuum model.

The likelihood ratios indicated that the discrete Markov model was about e^{25} and e^{139} times more likely than the fractal continuum model for the open and shut distributions, respectively, for the data in Fig. 2. Considering the open and shut distributions separately allows for the possibility that different mechanisms (models) might generate the open and shut times. If it is assumed that the basic mechanism generating open and shut times is the same, then the likelihood that each model described both the open and shut distributions is given by the product of the likelihoods of the separate open and shut distributions. (In practice, the natural logarithms of the separate likelihoods for the open and shut distributions are added.) When this was done the likelihood ratio indicated that the discrete Markov model was e^{164} (10^{71}) times more likely than the fractal continuum model for the data shown in Fig. 2.

Ranking the Models Taking into Account the Numbers of Free Parameters. Although the discrete Markov model was many times more likely than the fractal continuum model, as indicated by the likelihood ratio, such a comparison does not take into account the difference in the number of free parameters between the two models. Therefore, the Akaike predictor ranking, which applies a penalty for each additional free parameter, was used to rank the two models (Eq. 4 in the Methods). With this test, the model must be at least e-fold more likely for each additional free parameter for the model to maintain a higher ranking.

For Fig. 2, the discrete Markov model had five free parameters for each distribution (Eq. 2 in Methods), or three more than the fractal continuum model (Eq. 3). The Akaike predictor values for comparing the discrete Markov to the fractal continuum model for the data in Fig. 2 were 22 and 136 for the open and shut times considered separately, and 158 when considered together. These values were calculated with Eq. 4 by subtracting the difference in free parameters for the two models from the natural logarithm of the likelihood ratios. As these Akaike predictor values are greater than 0, the discrete Markov model still ranks above the fractal continuum model when the difference in free parameters is taken into account.

The Significance of the Rankings. A limitation of the Akaike predictor test is that the significance of the ranking is unknown. In order to set a significance level for the ranking of the discrete Markov model over the fractal continuum model, resampling methods detailed in Efron (1982) and Horn (1987) were used. Fig. 3 plots histograms

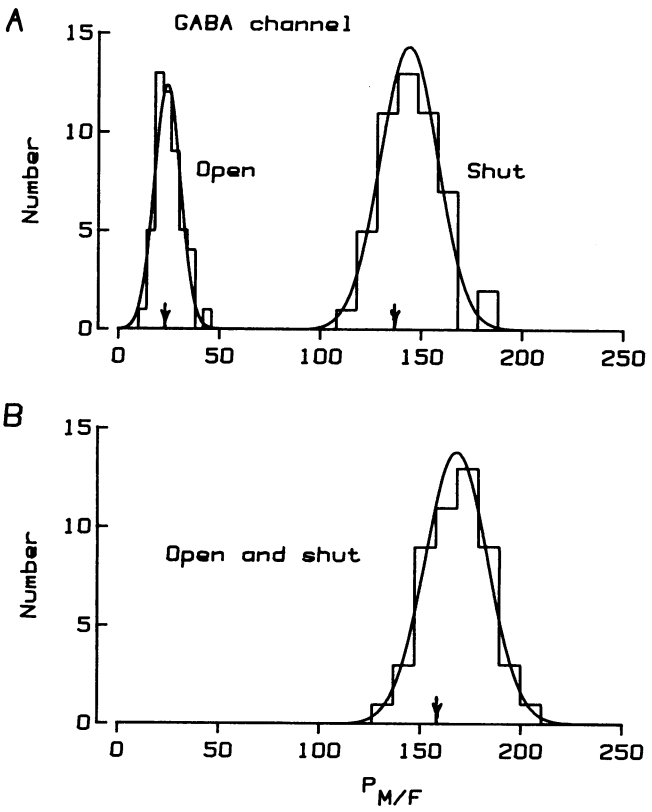

FIGURE 3 Histograms of Akaike predictor values comparing Markov and fractal models for the data in Fig. 1 from GABA-activated channels. The Markov and fractal models were fit to 51 resamples of the open and 51 resamples of the shut distributions shown in Fig. 2. (*A*) Akaike predictor values for resampled data were calculated with Eq. 4 and plotted as separate histograms for the open and shut times. (*B*) Akaike predictor values for resampled data are plotted for the open and shut distribution from each experiment considered together. The continuous lines are Gaussian distributions, with a mean of 24.1 and standard deviation of 6.45 for the open times, a mean of 143.7 and SD of 14.2 for the shut times, and a mean of 168 and an SD of 15.5 for the open and shut times considered together. The arrows indicate the Akaike predictor values of the original data.

of the Akaike predictor values for the distributions of open and shut intervals in Fig. 2 considered separately (*A*) and jointly (*B*) for 51 resamples of the original data (details in Methods). The histograms plot estimates of the expected variability in the predictor values if the experiment were performed 51 times. The arrows indicate the Akaike predictor values for the original data. The histograms show that the distributions of expected Akaike predictor values for the data in Fig. 2 clearly exceed zero.

The continuous lines plot Gaussian distributions describing the resampled data (see figure legend). The probability of Akaike predictor values of zero or less being obtained by chance alone from the Gaussian distributions would be $<10^{-4}$ for the open times, $<10^{-23}$ for the shut times, and $<10^{-27}$ for the open and shut distributions considered together. Hence, with a Gaussian assumption, the rankings of the discrete Markov model above the fractal continuum model for either separate or combined distributions were highly significant.

Summary of Data for GABA-activated Channels. Four different sets of open and shut intervals were analyzed for GABA-activated channels. In all four the discrete Markov model gave excellent descriptions of the open and shut times, and the fractal continuum model gave poorer descriptions, as indicated by the likelihood ratios.

When the differences in free parameters were taken into account with the Akaike test, and resampling was used to determine significance, the discrete Markov model ranked significantly above the fractal continuum model for three of the four shut data sets, with the ranking for the fourth data set being insignificant. Similar analysis showed that the discrete Markov model also ranked above the fractal continuum model for three of the four open data sets, but resampling indicated that only one of these rankings was significant.

When the open and shut data were considered jointly, the discrete Markov model ranked significantly above the fractal continuum for data from three of the four channels, with the ranking for the fourth channel being insignificant.

End-plate Channel

Fig. 4 presents log-log plots of the distributions of open (*A*) and shut (*B*) interval durations for data recorded from end-plate channels activated by 0.1 μM dihydroisoarecolone methiodide, a potent acetylcholine receptor agonist (Waters et al., 1988). Data are from six cell attached patches at the end-plate region of frog interosseal muscle. Similar to the findings for GABA-activated channels, the distributions of open and shut interval durations displayed inflections inconsistent with the fractal continuum model. As might be expected for data with inflections, the discrete Markov model gave excellent descriptions of the data (*continuous lines*), whereas the fractal continuum model

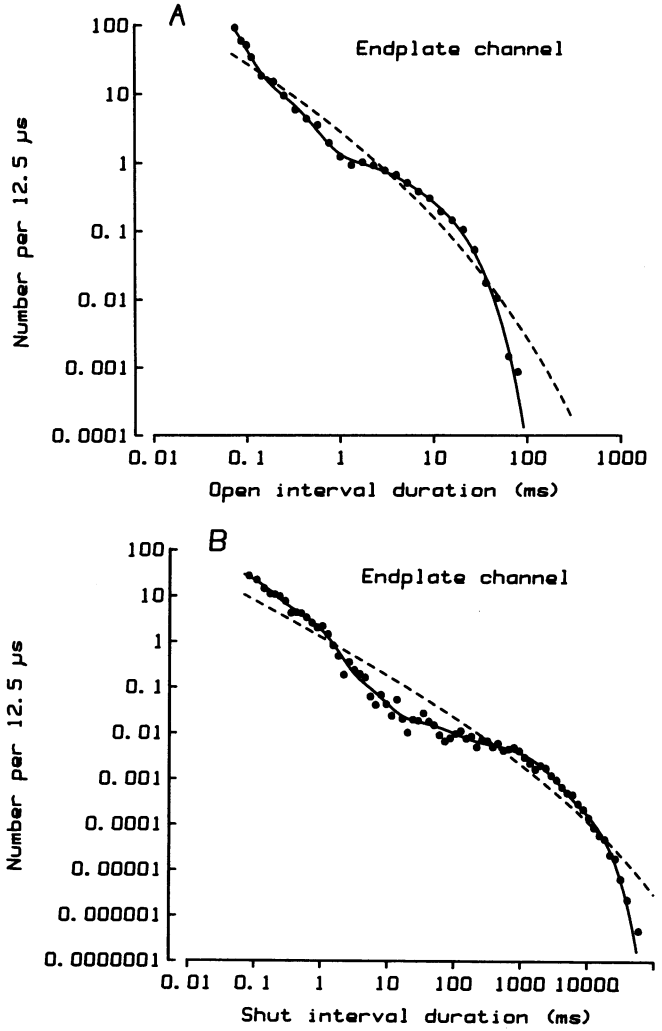

FIGURE 4 Distributions of open and shut interval durations recorded from endplate channels activated by 0.1 μM dihydroisoarecolone methiodide fit by Markov and fractal models. (*A*) Open times. The continuous line plots the maximum likelihood fit to the open durations with the sum of four exponentials, with time constants (and areas) of: 0.028 ms (0.656), 0.211 ms (0.130), 2.91 ms (0.057), and 11.0 ms (0.158). The dashed line plots the maximum likelihood fit to the open durations with the fractal continuum model, with $A = 2.88$ Hz$^{0.29}$ and $D = 1.71$. (*B*) Shut times. The continuous line plots the fit to the shut times with the sum of six exponentials, with time constants (and areas) of: 0.079 ms (0.167), 0.600 ms (0.201), 3.79 ms (0.0469), 62.2 ms (0.0428), 1,350 ms (0.346), and 6,680 ms (0.197). The dashed line plots the fit to the shut durations with the fractal continuum model, with $A = 0.360$ Hz$^{0.25}$ and $D = 1.75$. The likelihood ratio of Markov to fractal models was e^{160} for the open distribution and e^{463} for the shut. 1,217 open and 1,720 shut intervals were fitted and plotted.

gave poor descriptions (*dashed lines*). The inadequate fit by the fractal continuum model is reflected in the Akaike predictor values of 155 and 457 for the open and shut data sets, respectively, ranking the discrete Markov over the fractal continuum model (Eq. 4).

Similar results were found for end-plate channels activated by isoarecolone methiodide, another acetylcholine receptor agonist (Waters et al., 1988). These findings for

end-plate channels are in agreement with the data shown in Sigworth and Sine (1987), where the distribution of shut intervals for receptor channels activated by acetylcholine display a series of marked peaks, which are consistent with a discrete Markov model and not a fractal continuum model.

Fast Cl Channel

Fig. 5 presents log-log plots of the distributions of open (*A*) and shut (*B*) interval durations for data recorded from a single fast Cl channel in an excised membrane patch from cultured rat skeletal muscle. Similar to, but even more pronounced than for the GABA and end-plate channels, the distribution of shut interval durations displayed marked inflections. The distribution of open interval durations displayed, at most, only a minor inflection, suggesting a smaller fraction of open intervals of briefer duration than for the GABA and end-plate channels. (The areas of the exponential components are in the figure legend.)

The discrete Markov model gave excellent descriptions of both the open and shut distributions (*continuous lines*). The fractal continuum model gave a slightly worse description of the open times than the discrete Markov, as indicated by the likelihood ratio (Markov to fractal) of 3.1. By taking into account the greater number of free parameters for the discrete Markov model, the Akaike predictor value (Eq. 4) was 0.1, which was not significantly different from zero. The fractal continuum model gave a very poor description of the shut times (*dashed lines*), as indicated by the Akaike predictor value of 952.

For 11 additional open distributions from single fast Cl channels, including the data presented in Blatz and Magleby (1986*b*), results similar to those shown in Fig. 5 *A* were found. The discrete Markov model gave excellent descriptions of the open times, and the descriptions of the open times by the fractal model appeared (by visual inspection) as good. The likelihood ratios indicated somewhat greater errors for the fractal model, however. When the larger number of free parameters for the Markov model were taken into account, the Akaike predictor values clustered around zero. Resampling indicated only one significant ranking in the 12 open distributions, and in that case the Markov model ranked below the fractal, with a P value of 0.045. Such a ranking would be expected by chance alone about once every 20 distributions, even if the rankings of the two models were not significantly different.

For all 12 shut distributions examined from the fast Cl channel, the Markov model ranked significantly above the fractal model, and the likelihood ratios usually exceeded e^{900}. Such high likelihood ratios arose because typically more than 95% of the tens of thousands of intervals in the shut distributions were described with errors greater than 20–1,000% by the fractal continuum model. If the open and shut data sets were considered jointly, then the Akaike test ranked the Markov model significantly above the fractal for all 12 data sets consisting of open and shut distributions.

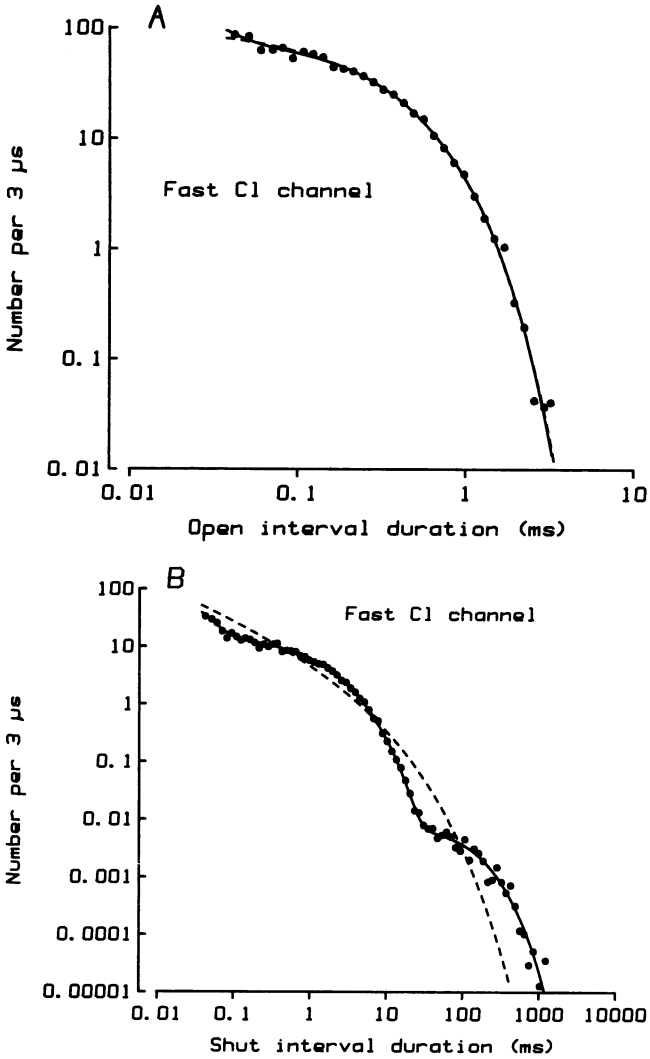

FIGURE 5 Distributions of open and shut interval duraitons recorded from the fast Cl channel fit by Markov and fractal models. (*A*) Open times. The continuous line plots the maximum likelihood fit to the open durations with the sum of three exponentials, with time constants (and areas) of: 0.013 ms (0.168), 0.208 ms (0.233), and 0.403 ms (0.599). The dashed line plots the maximum likelihood fit to the open times with the fractal continuum model, with $A = 1430\ \text{Hz}^{0.92}$ and $D = 1.08$. (*B*) Shut times. The continuous line plots the fit to the shut durations with the sum of six exponentials, with time constants (and areas) of: 0.024 ms (0.106), 0.362 ms (0.0737), 1.63 ms (0.421), 4.32 ms (0.359), 111 ms (0.0247), and 229 ms (0.0153). The dashed line plots the fit to the shut durations with the fractal continuum model, with $A = 6.22\ \text{Hz}^{0.43}$ and $D = 1.57$. The likelihood ratios of the Markov to fractal model were $e^{3.1}$ for the open distribution and e^{961} for the shut. 7,810 open and 7,996 shut intervals were fitted and plotted. Membrane potential, −90 mV; temperature, 22°C.

The Large Conductance Ca-Activated K Channel (BK Channel)

McManus and Magleby (1988) have shown that the distributions of open and shut interval durations recorded from single BK channels display inflections, consistent

with discrete states. They found that the discrete Markov model described the open and shut distributions for the BK channel, whereas the fractal continuum model could not describe either open or shut distributions. In the three data sets they examined, including the one plotted in Figs. 11 and 12 in McManus and Magleby (1988), the Akaike predictor value ranked the discrete Markov model above the fractal continuum model for both the open and shut distributions, considered separately or jointly.

We have examined an additional 15 data sets for the BK channel, and found inflections consistent with discrete states, excellent fits by the Markov model, typically poor fits by the fractal model, and Akaike predictor values which always ranked the discrete Markov model over the fractal continuum model. Resampling suggested that the rankings were significant for all 18 shut data sets and for 16 of the 18 open data sets. The two open data sets where the rankings were not significant were of smaller sample sizes. When the open and shut data were considered jointly, all rankings were significant. Activity during the different kinetic modes of the BK channel (see McManus and Magleby, 1988) was also best fit by discrete Markov models (not shown).

Further evidence suggesting that the fractal continuum model does not describe the kinetics of BK channels, are the observations of Korn and Horn (1988). They find that the discrete Markov model ranks significantly above the fractal continuum model for open times recorded from a Ca-activated K channel in GH_3 pituitary cells.

Akaike Predictor Values for Four Channels

Fig. 6 *A* summarizes the ranking of discrete Markov to fractal continuum models for 36 open (*open symbols*) and 36 shut time distributions, obtained from four different channels. Fig. 6 *B* plots rankings if the open and shut times in a data set are ranked together. The Akaike predictor value, $P_{M/F}$ given by Eq. 4, is plotted against the number of intervals analyzed. The discrete Markov model ranks above the fractal continuum model if $P_{M/F} > 0$. In each figure the dashed lines enclose the data points with insignificant rankings. In 54 of 72 distributions of open and shut times considered separately, the Markov model ranked above the fractal, in 17 there were no significant differences, and in one the Markov model ranked below the fractal (Fig. 6 *A*). In 35 of 36 evaluations of open and shut times considered together, the Markov model ranked significantly above the fractal, and in the one remaining evaluation there was no significant difference.

Notice that the data in Fig. 6 are plotted on double logarithmic coordinates, and from Eq. 4 that the Akaike predictor value, $P_{M/F}$ is an exponent. Thus, for the data sets where the two models are not significantly different (those between the dashed lines), and the one data set where the fractal model ranked above the Markov, the ranking values differed by less than e^2. In contrast, in all the remaining data sets the Markov model was e^{10} to $e^{10,000}$ times more likely.

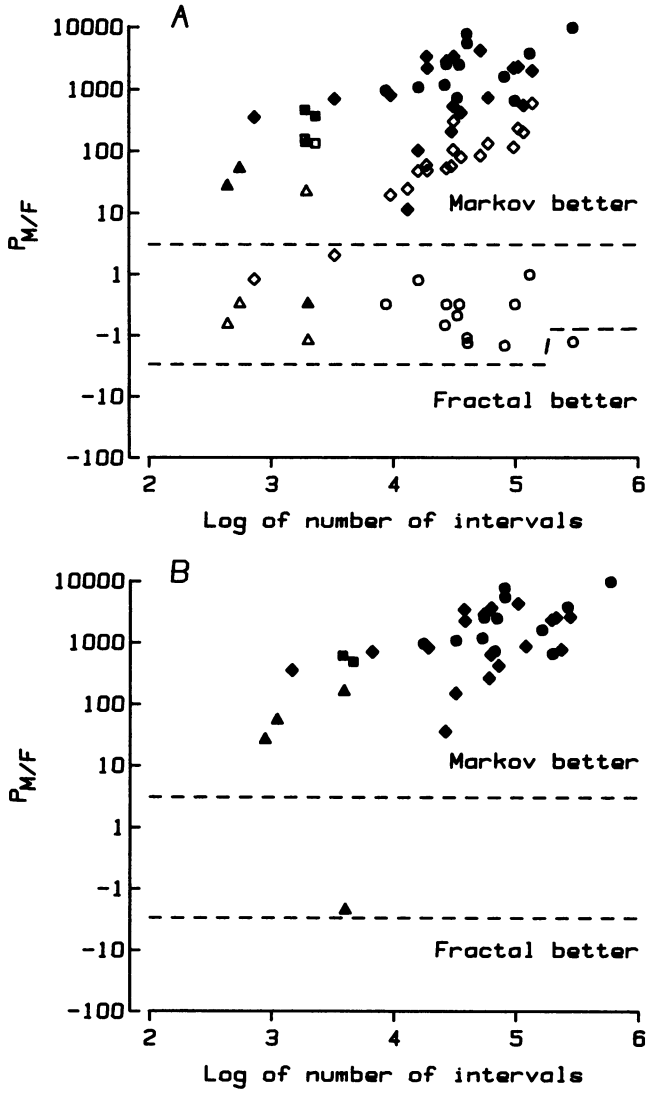

FIGURE 6 Ranking of discrete Markov to fractal continuum model for 36 data sets of open and shut intervals from four different types of channels. (*A*) Akaike predictor values ($P_{M/F}$) for open and shut distributions considered separately are plotted against the number of events in each distribution. Open and filled symbols are for open and shut distributions, respectively. (*B*) Akaike predictor values determined for each data set, with the open and shut distribution considered together, are plotted against the number of open and shut intervals in the data set. Data from: GABA-activated channels, *triangles;* endplate channels, *squares;* fast Cl channels, *circles;* and large conductance calcium-activated potassium channels, *diamonds*. The rankings of points falling between the dashed lines were not significantly different from zero.

Distinguishing Models with the Chi-Squared Goodness of Fit Test

Some comparisons of fits by the discrete Markov and fractal continuum model were also made using the Chi-squared goodness of fit test, where the number of degrees of freedom, m, was calculated from: $m = b - 1 - p$, where

b is the number of bins, and p the number of free parameters in the fit. The two open and two shut distributions from the end-plate channel and the first eight open and eight shut distributions from the BK channel were analyzed. The findings were consistent with those in Fig. 6. In all 20 distributions, the Chi-squared goodness of fit test indicated that the observed data were consistent ($P > 0.05$) with the discrete Markov model. In contrast, in 18 of the 20 distributions the Chi-squared test indicated that the data were inconsistent with the fractal continuum model, and in each of these 18 distributions the P values were <0.001 that the data were generated by a fractal model. For the same 20 distributions, the Akaike predictor test and resampling ranked the Markov model significantly above the fractal in 19, with one of the 19 being just significant, and no significant difference was found for one distribution. Thus, the Chi-squared test and Akaike test with resampling gave similar results, and the results of these two tests simply confirmed in a quantitative manner the same conclusions which could be drawn from visual inspection of the fits to the data.

DISCUSSION

Liebovitch et al. (1987) and Liebovitch and Sullivan (1987) have recently considered the possibility that the distributions of interval durations from single channels may be consistent with an empirical fractal scaling equation. Their interpretation of the empirical equation is that gating kinetics of single channels are consistent with a continuum of states, with the effective rate constants for leaving the collections of open and shut states consistent with fractal scaling. Such a fractal continuum gating mechanism for single channels is in marked contrast to discrete Markov models which assume discrete states, with the transition rates between the states remaining constant in time (see Colquhoun and Hawkes, 1981; Hille, 1984). As discrete Markov and fractal continuum models imply fundamental differences in the gating mechanisms of ion channels, and consequently, projected differences in the observed single channel kinetics, critical analysis of the single channel data should allow these two models to be distinguished.

Since it has already been established that discrete Markov models account for many properties of single channel kinetics (Neher and Sakmann, 1976; Moczydlowski and Latorre, 1983; Aldrich et al., 1983; Horn and Vandenberg, 1984; Colquhoun and Sakmann, 1985; Blatz and Magleby, 1986*b*; Sine and Steinbach, 1987; McManus and Magleby, 1988), we examined whether the fractal continuum model could also describe single channel kinetics, and determined which of these two models was more probable. Four different types of ion channels were examined: GABA-activated channels, end-plate channels, fast Cl channels, and large conductance Ca-activated K channels.

To evaluate the relative abilities of the two models to describe the data, we have compared the fits by the fractal continuum model against those by the discrete Markov model using an Akaike predictor value to rank the models, and resampling to determine the significance of the rankings. The Akaike predictor value applies a heavy penalty for free parameters; each additional free parameter must increase the probability at least e-fold for a ranking to remain unchanged (Eq. 4). The Chi-squared goodness of fit test was also used to compare models to the data for two of the channels and, in general, gave results consistent with the Akaike predictor values and resampling.

Comparison of Discrete Markov and Fractal Continuum Models

36 data sets were examined, each containing a distribution of open times and a distribution of shut times. The best possible description of the data by each model was determined by maximum likelihood methods, and the fits were quantified by calculating the probability that the observed data were generated by each model.

In all 72 distributions of open and shut times considered separately, discrete Markov models gave excellent descriptions of the data. In contrast, in 54 of the distributions the fractal continuum model gave poor descriptions of the data, in 16 open and one shut distribution there were no significant differences between the two models, and in one open distribution the Markov model ranked below the fractal (Fig. 6 *A*). For those distributions where the ranking of the models was not significant and in the one open distribution where the fractal model ranked higher, the fits with the Markov model had less error, but had lower rankings due to the greater number of free parameters. Treating the open and shut distributions separately in this manner allows the possibility that different models may account for gating motions in the open and shut states of the same channel.

If it is assumed that the same model must account for gating motions in proteins for both the open and shut states, then in 35 of the 36 data sets, the discrete Markov model ranked significantly above the fractal continuum model (Fig. 6 *B*). In the remaining data set, the ranking was not significant. The best fits by the fractal model often resulted in errors between the observed and predicted shut distributions of hundreds to thousands of percent (*dashed lines*, Figs. 2, 4, and 5). Furthermore, the fractal model was usually hundreds to thousands of orders of magnitude less probable than discrete Markov models (Fig. 6). These likelihood differences and poor fits suggest that the fractal continuum model is inadequate as a general mechanism for the gating of these four channels.

However, the fractal model did describe the open times for the fast Cl channel as well as the Markov model (Fig. 5 *A*; *open circles*, Fig. 6 *A*), and therefore, the question arises of whether the fractal model might be preferred in this

case. We think not for the following reasons: (*a*) as pointed out by Millhauser et al. (1988), the fractal model leads to infinitely large rate constants at zero time and, therefore, is not consistent with modern views of quantum chemistry; (*b*) the simplicity of the fractal model will be lost when it is expanded to account for the inverse relationship observed by McManus et al. (1985) between the durations of adjacent open and shut intervals; (*c*) since the Markov model is consistent with both the open and shut times, whereas the fractal model is consistent with only the open times, it seems most economical to assume that the open times are described by the same basic mechanism as the shut times.

Since the fractal continuum model appears consistent with the data examined in its initial consideration (Liebovitch et al., 1987; Liebovitch and Sullivan, 1987), the question arises, then, whether Markov models might be inconsistent with the same data, as the channels examined to develop the fractal model were different from the ones examined in this paper. A definitive answer is not possible without further analysis, but several factors suggest that a Markov model would be ranked equal to or higher than a fractal model for the channels examined to develop the fractal model.

(*a*) The limited time resolution of 1–1.6 ms in the data examined by Liebovitch et al. (1987) and Liebovitch and Sullivan (1987) would have masked a part of the distributions where major deviations from fractal kinetics often occur, as indicated by Figs. 2, 4, and 5 in this study, Figs. 11 and 12 in McManus and Magleby (1988), and the data in Korn and Horn (1988).

(*b*) Liebovitch et al. (1987) found that the fractal and Markov models gave similar descriptions of their data. We have analyzed the same data from their Fig. 4 and found similar results; the ranking of the models was not significant (although the Akaike predictor value did rank the Markov over the fractal model). More detailed analysis by Korn and Horn (1988) indicates that the inability to discriminate between the two models is due to the limited sample size, and not the fact that the models are indistinguishable.

(*c*) A requirement of fractal kinetics is that the data be self similar on different time scales. Liebovitch and Sullivan (1987) have tested for self similarity by plotting data on different time scales. Although the data approximate self similarity, some pronounced differences between the plots suggest deviation from a fractal model. Thus, a Markov model may well give a better description of the data.

Discrete Kinetic States

The discrete bumps and inflections in log-log plots of open and shut times (Blatz and Magleby, 1986*b*; Sigworth and Sine, 1987; Horn, 1987; Kerry et al., 1988; McManus and Magleby, 1988; Korn and Horn, 1988) suggest that single channels pass through discrete kinetic states during gating, as required for discrete Markov models, rather than a continuum of states, as required for the fractal continuum model. Multiple bumps and inflections in log-log distributions of interval durations, although not always prominent, are such a general feature of single channel kinetics that models which cannot generate such bumps and inflections can be excluded from consideration as general gating mechanisms. It should also be noted that the absence of discrete bumps and inflections in log-log plots of interval durations are not inconsistent with discrete states. Sums of exponentials, as required for discrete Markov models, can generate either bumps or apparently smooth curves on log-log plots, depending on the exponential parameters (Fig. 1).

The finding of data consistent with discrete kinetic states in our study should not be surprising, as three of the four channels studied are activated by the binding of agonist or Ca. The binding of each additional agonist molecule would add an additional distinct chemical state. Since the time spent in these different chemical states might be expected to affect the durations of the open and shut intervals, then these chemical states could give rise to distinct kinetic states (Colquhoun and Hawkes, 1981; McManus and Magleby, 1988).

In light of the hundreds of amino acids and resulting large proteins that form channel molecules (c.f. Finer-Moore and Stroud, 1984; Noda et al., 1984), it might be expected that there would be a large number of conformational states (see references in Liebovitch et al., 1987). Why then, are there so few kinetic states? Some conformations may simply have little, if any, effect on the gating associated with the opening and closing of the channel. Other conformations may have lifetimes too brief or too long or too similar in duration to be detected as distinct kinetic states within the resolution of the kinetic analysis of the data. Finally, each kinetic state may arise from many conformational substates which equilibrate rapidly enough (c.f. Ansari et al., 1985) that they are not detected by single channel analysis techniques.

Models Based on Idealized Assumption of Protein Dynamics

Although our data suggest that the simple fractal continuum model of Liebovitch et al. (1987) cannot serve as a general model for the gating of four different channels, the fractal model was one of the first to explore gating properties based on the notion that the time course of dynamic processes in proteins can occur over many orders of magnitude. The observations of Liebovitch et al. (1987) and Liebovitch and Sullivan (1987), that distributions of shut times can be approximated by a power type function, and their concept of considering gating in terms of idealized assumptions about protein dynamics has led to two interesting models for channel gating. Both models are discrete Markov models, but they differ from more traditional discrete Markov models in that they have a very

large number of states, rather than the fewest possible states, and it is assumed that the rates constants for transitions among the states are similar (Millhauser et al., 1988; Laüger, 1988).

The expansion of these many-state models to include multiple independent transition pathways between open and shut states and also to include some rate constants which are slower than the uniform rate constants, should allow them to provide descriptions of single channel kinetics equivalent to those presently obtained from discrete Markov models with fewer states. Thus, the potential contribution of the protein dynamics approach upon which the many-state models are based is not that the resulting models will have fewer free parameters, but that the approach provides a means to study gating by starting at the opposite end of the question asked by the more traditional kinetic approach. The protein dynamics approach explores which assumptions about protein dynamics are consistent with the observed data. The traditional kinetic approach explores which kinetic gating mechanisms are consistent with the observed data. Proper application of both approaches should speed our understanding of channel gating.

We thank Dr. Larry Liebovitch for many highly stimulating discussions and for kindly providing us with the data in Fig. 4 of Liebovitch et al. (1987).

This work was supported in part by grants from the National Institutes of Health (AR-32805) and the Muscular Dystrophy Associaton, O. B. McManus has received fellowships from the Muscular Dystrophy Association and the National Institutes of Health (NIH) (NS-07044). D. S. Weiss holds a fellowship from the NIH (NS-08138).

Received for publication 11 March 1988 and in final form 18 July 1988.

REFERENCES

Akaike, H. 1974. A new look at statistical model identification. *IEEE Trans. Auto. Control.* AC-19:716–723.

Aldrich, R. W., D. P. Corey, and C. F. Stevens. 1983. A reinterpretation of mammalian sodium channel gating based on single channel recording. *Nature (Lond.).* 306:436–441.

Ansari, A., J. Berendzen, S. F. Bowne, H. Frauenfelder, I. E. T. Iben, T. B. Sauke, E. Shyamsunder, and R. D. Young. 1985. Protein states and proteinquakes. *Proc. Natl. Acad. Sci. USA.* 82:5000–5004.

Blatz, A. L., and K. L. Magleby. 1986*a*. Correcting single channel data for missed events. *Biophys. J.* 49:967–980.

Blatz, A. L., and K. L. Magleby. 1986*b*. Quantitative description of three modes of activity of fast chloride channels from rat skeletal muscle. *J. Physiol. (Lond.).* 378:141–174.

Colquhoun, D., and A. G. Hawkes. 1981. On the stochastic properties of single ion channels. *Proc. R. Soc. Lond. B Biol.* 211:205–235.

Colquhoun, D., and F. J. Sigworth. 1983. Fitting and statistical analysis of single-channel records. *In* Single-Channel Recording. B. Sakmann and E. Neher, eds. Plenum Press, New York. 191–263.

Colquhoun, D., and B. Sakmann. 1985. Fast events in single-channel currents activated by acetylcholine and its analogues at the frog muscle end-plate. *J. Physiol.* 369:501–557.

Efron, B. 1982. The Jackknife, the Bootstrap, and Other Resampling Plans. Society for Industrial and Applied Mathematics, Philadelphia.

Finer-Moore, J., and R. M. Stroud. 1984. Amphipathic analysis and possible formation of the ion channel in an acetylcholine receptor. *Proc. Natl. Acad. Sci. USA.* 81:155–159.

Hamill, O. P., A. Marty, E. Neher, B. Sakmann, and F. J. Sigworth. 1981. Improved patch clamp techniques for high-resolution current recording from cells and cell-free membrane patches. *Pfluegers Arch.* 391:85–100.

Hille, B. 1984. Ionic Channels of Excitable Membranes. Sinauer Associates Inc., Sunderland.

Horn, R. 1987. Statistical methods for model discrimination: application to gating kinetics and permeation of the acetylcholine receptor channel. *Biophys. J.* 51:255–263.

Horn, R., and K. Lange. 1983. Estimating kinetic constants from single channel data. *Biophys. J.* 43:207–223.

Horn, R., and C. A. Vandenberg. 1984. Statistical properties of single sodium channels. *J. Gen. Physiol.* 84:505–534.

Kerry, C. J., R. L. Ramsey, M. S. P. Sansom, and P. N. R. Usherwood. 1988. Glutamate receptor channel kinetics. The effect of glutamate concentration. *Biophys. J.* 53:39–52.

Korn, S. J., and R. Horn. 1988. Statistical discrimination of fractal and Markov models of single channel gating. 54:871–877.

Labarca, P., J. A. Rice, D. R. Fredkin, and M. Montal. 1985. Kinetic analysis of channel gating. Application to the cholinergic receptor channel and the chloride channel from *Torpedo californica. Biophys. J.* 47:469–478.

Laüger, P. 1988. Internal motions in proteins and gating kinetics of ionic channels. *Biophys. J.* 53:877–884.

Liebovitch, L. S., and J. M. Sullivan. 1987. Fractal analysis of a voltage-dependent potassium channel from cultured mouse hippocampal neurons. *Biophys. J.* 52:979–988.

Liebovitch, L. S., J. Fischbarg, J. P. Koniarek, I. Todorova, and M. Wang. 1987. Fractal model of ion-channel kinetics. *Bioch. Biophys. Acta.* 896:173–180.

Magleby, K. L., and B. S. Pallotta. 1983. Calcium-dependence of open and shut interval distributions from calcium-activated potassium channels in cultured rat muscle. *J. Physiol. (Lond.).* 344:585–604.

Magleby, K. L., O. B. McManus, D. S. Weiss, A. L. Blatz, and C. E. Spivak. 1988. Discrete Markovian models ranked above fractal models for single channel kinetics of large conductance calcium-activated potassium channel, GABA-activated channel, fast chloride channel, and acetylcholine receptor channel. *Biophys. J.* 53:462a. (Abstr.)

McManus, O. B., and K. L. Magleby. 1988. Kinetic states and modes of single large-conductance calcium-activated potassium channels in cultured rat skeletal muscle. *J. Physiol. (Lond.).* 402:79–120.

McManus, O. B., A. L. Blatz, and K. L. Magleby. 1985. Inverse relationship of the durations of adjacent open and shut intervals for Cl and K channels. *Nature (Lond.).* 317:625–628.

McManus, O. B., A. L. Blatz, and K. L. Magleby. 1987. Sampling, log binning, fitting, and plotting durations of open and shut intervals from single channels and the effects of noise. *Pfluegers Arch.* 410:530–553.

Miller, C. 1983. Integral membrane channels: studies in modal membranes. *Physiol. Rev.* 63:1209–1242.

Millhauser, G. L., E. E. Salpeter, and R. E. Oswald. 1988. Diffusion models of ion-channel gating and the origin of power-law distributions from single-channel recording. *Proc. Natl. Acad. Sci. USA.* 85:1503–1507.

Moczydlowski, E., and R. Latorre. 1983. Gating kinetics of Ca^{2+}-activated K^+ channels from rat muscle incorporated into planar lipid bilayers: evidence for two voltage-dependent Ca^{2+} binding reactions. *J. Gen. Physiol.* 82:511–542.

Neher, E., and B. Sakmann. 1976. Single-channel currents recorded from membrane of denervated frog muscle fibers. *Nature (Lond.).* 260:799–802.

Noda, M., S. Shimizu, T. Tanabe, T. Takai, T. Kayano, T. Ikeda, H. Takahashi, H. Nakayama, Y. Kanaoka, N. Minamino, K. Kangawa, H. Matsuo, M. A. Raftery, T. Hirose, S. Inayama, H. Hayashida, T. Miyata, and S. Numa. 1984. Primary structure of *Electrophorus*

electricus sodium channel deduced from cDNA sequence. *Nature (Lond.)*. 312:121–127.

Rao, C. R. 1973. Linear Statistical Inference and its Applications. John Wiley & Sons, Inc., New York.

Roux, B, and R. Sauvé. 1985. A general solution to the time interval omission problem applied to single channel analysis. *Biophys. J.* 48:149–158.

Sigworth, F. J., and S. M. Sine. 1987. Data transformations for improved display and fitting of single-channel dwell time histograms. *Biophys. J.* 52:1047–1054.

Sine, S. M., and J. H. Steinbach. 1987. Activation of acetylcholine receptors on clonal mammalian BC 3H-1 cells by high concentrations of agonist. *J. Physiol. (Lond.)*. 385:325–359.

Waters, J. A., C. E. Spivak, M. Hermsmeier, J. S. Yadav. R. F. Liang, and T. M. Gund. 1988. Synthesis, pharmacology and molecular modeling studies of semirigid, nicotinic agonists. *J. Med. Chem.* 31:545–554.

Weiss, D. S. 1988. Membrane potential modulates the activation of GABA-gated channels. *J. Neurophysiol.* 59:514–527.

Weiss, D. S., E. M. Barnes, Jr., and J. J. Hablitz. 1988. Whole-cell and single-channel recordings of GABA-gated currents in cultured chick cerebral neurons. *J. Neurophysiol.* 59:495–513.